Transitional Velocity Patterns in a Smooth Concentric Annulus

J. E. WALKER and R. R. ROTHFUS

Carnegie Institute of Technology, Pittsburgh, Pennsylvania

Profiles of mean local velocities have been experimentally determined in a smooth, concentric, horizontal annulus having a radius ratio of 0.331. The test fluid was water at room temperature flowing steadily at Reynolds numbers in the viscous, transition, and lower turbulent ranges. The transitional profiles, obtained by means of an impact probe, are summarized and discussed. Limits of the transition zone are established, and variation of the radius of maximum velocity with Reynolds number is confirmed.

Relatively little is known about laminar-turbulent transition in concentric annuli. There is published information about fluid friction in this region but no adequate indication of what velocity patterns are to be expected. The present investigation has been undertaken as a first step in determining the effect of Reynolds number on the transitional velocity profiles. A calibrated impact probe has been used to obtain mean local velocities in water flowing steadily and isothermally through a smooth, horizontal annulus having a radius ratio of 0.331. Data have been obtained at various Reynolds numbers from 250 to 10,000 with most attention centered on the transition zone.

The pressure-drop data supplementing the present velocity measurements have already been reported by Walker, Whan, and Rothfus (*7*). The correlated results on pressure drop cover the entire range of radius ratios from zero to unity. The data indicate that the extent of the transition region on the Reynolds-number scale depends to some degree on the radius ratio. For the radius ratio examined herein, namely 0.331, the major transitional changes in the curve of Fanning friction factor against Reynolds number occur at Reynolds numbers between 2,200 and 3,100.

The frictional data have been correlated in terms of the Reynolds number

$$N_{Re_2} = \frac{2(r_2^2 - r_m^2)}{r_2} \frac{V\rho}{\mu} \qquad (1)$$

The characteristic length in this case is four times the hydraulic radius of that portion of the stream lying between the outer radius and the radius of maximum local velocity. The bulk average linear velocity is taken over the whole annular section between the outer radius and the inner or core radius. The cited friction factor in turn is the one at the outer wall of the annulus, defined as

$$f_2 = \frac{2\tau_2 g_c}{\rho V^2} \qquad (2)$$

The pressure-drop data show that the relationship between f_2 and N_{Re_2}, in fully turbulent flow, is coincident with the corresponding correlation for smooth tubes. Thus, the method of hydraulic radius can be applied to the portion of the annulus outside the radius of maximum velocity, regardless of the radius ratio. This is the reason for using the Reynolds number defined in Equation (1) when the frictional data are correlated.

The fully turbulent velocity profiles measured in the present experiments are reported in a paper by Rothfus, Walker, and Whan (*5*). A means of correlating these data with smooth-tube and parallel-plate profiles is described there. It appears that a successful method has been found for predicting fully turbulent velocity patterns, regardless of the radius ratio of the annulus. In addition the velocity data confirm observations of Rothfus, Monrad, and Senecal (*3*) and of Knudsen and Katz (*1*) that the radius of maximum velocity in full turbulence corresponds to that in fully viscous flow. The latter value is easily shown to be related to the annular dimensions through the equation

$$r_m^2 = (r_2^2 - r_i^2)/2 \ln (r_2/r_i) \qquad (3)$$

When the radius of maximum velocity is either unknown or of primary interest, it is convenient to correlate data in terms of the Reynolds number obtained by combing Equations (1) and (3).

Some direct measurements of the skin friction on the cores of annuli having radius ratios of 0.507 and 0.337 have been made by Rothfus, Monrad, Sikchi, and Heideger (*4*). From such data the friction factor at the inner wall of the annulus can be calculated from the defining equation

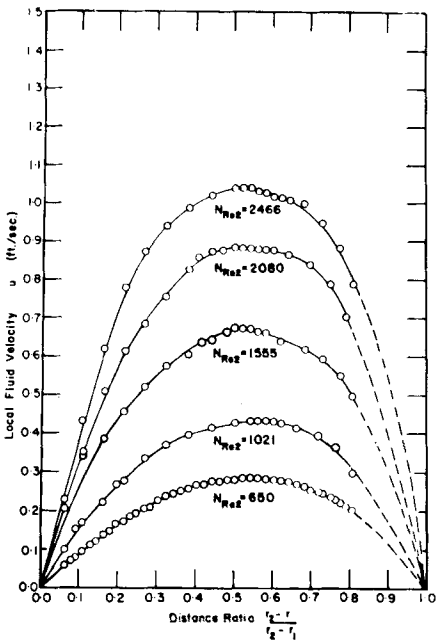

Fig. 1. Transitional velocity profiles for water at 20°C. flowing in a smooth annulus; radius ratio r_1/r_2 = 0.33.

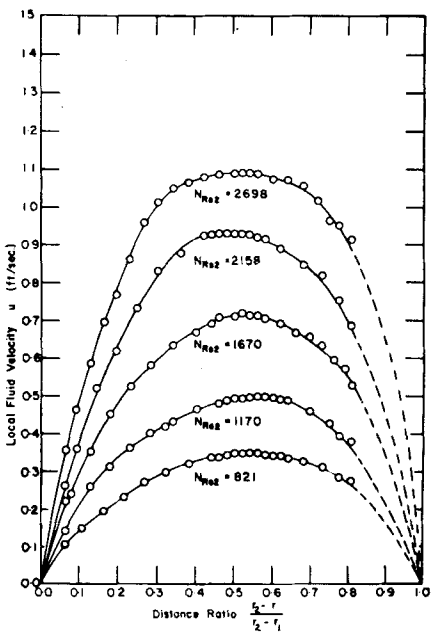

Fig. 2. Transitional velocity profiles for water at 20°C. flowing in a smooth annulus; radius ratio r_1/r_2 = 0.33.

J. E. Walker is at present with the Standard Oil Company of Louisiana, Baton Rouge, Louisiana.

The original data appear in a doctoral thesis by J. E. Walker which is available on interlibrary loan from Carnegie Institute of Technology, Pittsburgh, Pennsylvania.

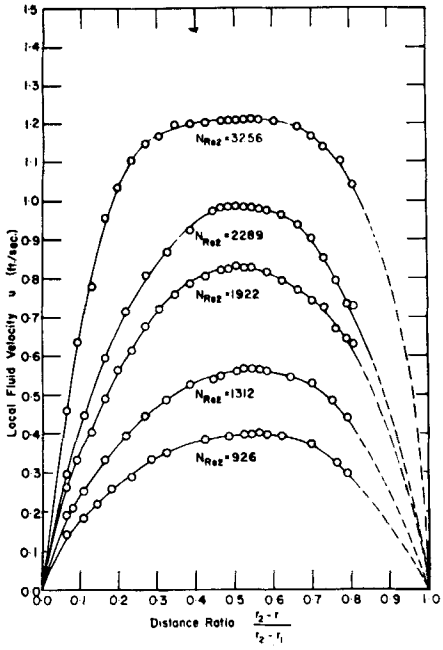

Fig. 3. Transitional velocity profiles for water at 20°C. flowing in a smooth annulus; radius ratio $r_1/r_2 = 0.33$.

$$f_1 = \frac{2\tau_1 g_c}{\rho V^2} \qquad (4)$$

Simple force balances on the fluid inside and outside the radius of maximum velocity show that

$$\frac{\tau_1}{\tau_2} = \frac{f_1}{f_2} = \frac{r_2}{r_1}\frac{(r_m^2 - r_1^2)}{(r_2^2 - r_m^2)} \qquad (5)$$

Since the force balances are independent of the flow regime, Equation (5) must involve the actual value of the radius of maximum velocity, whatever it may be. Thus if the flow is fully viscous or fully turbulent, r_m can be calculated by means of Equation (3). In the transition zone however r_m proves to have other values as shown in reference *4*, where the pressure-drop data of reference *3* were used in combination with the skin-friction data of reference *4* to obtain separate values of f_1 and f_2. Equation (5) was then utilized to determine the influence of Reynolds number on the radius of maximum velocity. The results indicated that a regular and appreciable deviation of r_m from its viscous-flow value occurred in the transition range. It consequently became a concern of the present investigation to verify such behavior through measurement of local fluid velocities.

EXPERIMENTAL EQUIPMENT

The experimental apparatus was basically a simple, open, hydraulic loop equipped with accessories for control of flow rate and temperature. Water at room temperature was circulated at steady rates which were measured by means of a calibrated volumetric tank. The test section for the velocity measurements consisted of 30 ft. of smooth brass conduit having a 0.750-in. I.D. which was fitted with a concentric, smooth, copper core of 0.248 in. diameter. The middle 3 ft. of the outer tube were replaced by a Lucite section having exactly the same inside diameter. The transparent tube, which was held in perfect alignment by a shouldered joint, permitted the position of the velocity probe to be checked visually from time to time. As the test section was horizontal, it was necessary to prevent sagging of the core by applying tension on the core through a screw mechanism.

The impact probe was a straight length of stainless steel hypodermic tubing having an outside diameter of 0.058 in. The probe was capped with 0.008-in. thick stainless steel, silver-soldered in place, and ground flush with the sides of the tubing. The impact opening, 0.020 in. in diameter, was drilled in the side of the probe with its edge approximately 0.003 in. from the capped end. The probe was attached to a feed mechanism which permitted the center of the impact opening to be positioned in the fluid stream with a precision of 0.001 in. Distances were measured from a reference point on a micrometer scale. The reference position was established by temporarily removing the core and permitting the probe to make contact with the opposite side of the outer tube.

The differences between the total pressure on the opening in the probe and the static pressure at the wall of the outer tube were measured by means of vertical U-tube manometers filled with carbon tetrachloride, monochlorobenzene, or monofluorobenzene, depending on the desired amplification of the readings. To maintain proper behavior of the liquid interfaces the manometers were carefully cleaned and a silicone layer was baked on their inner surfaces.

EXPERIMENTAL PROCEDURE

The test section was aligned by means of a transit theodolite, and the core diameter was measured after tension had been applied to eliminate appreciable sag. The impact probe was calibrated by the method of Stanton, Marshall, and Bryant (*6*). No investigation of calming length was made, since the impact probe was situated at a point where there were 725 equivalent diameters of calming length upstream from it and 676 equivalent diameters downstream.

In a typical run the flow rate was established and sufficient time allowed for steady state to be reached. Local velocities were then measured at various points in the fluid cross section. Approximately half an hour elapsed between successive settings of the probe position. The distance between successive positions and the direction of approach to them were varied both regularly and at random.

Enough data were taken to establish the relationship between the radius of maximum velocity and the Reynolds number. Additional measurements of the maximum velocity were then made at these radii. The relationship between the Reynolds number and the ratio of average to maximum velocity could thus be determined without measuring a full velocity profile at each flow rate.

Since the water was recycled by means of pumps, it tended to increase in temperature over long periods of operation. The temperature was held within 0.1°C. of a constant value, however, by the addition of a small amount of cold water to the system at intervals of approximately 1 hr. The water and room temperatures were kept essentially the same to assure isothermal flow in the test section.

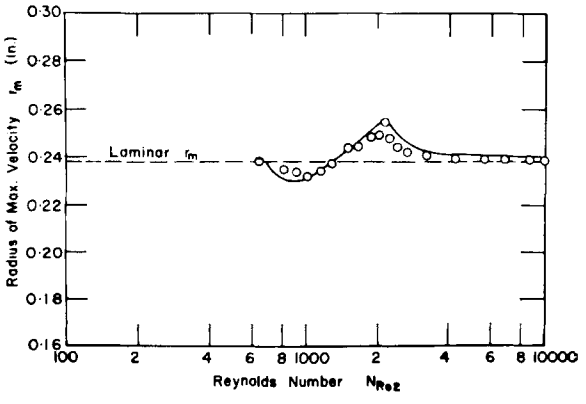

Fig. 4. Effect of Reynolds number on radius of maximum velocity; radius ratio $r_1/r_2 = 0.33$. (Solid line shows prediction based on pressure drop and drag measurements. Circles show experimental velocity data.)

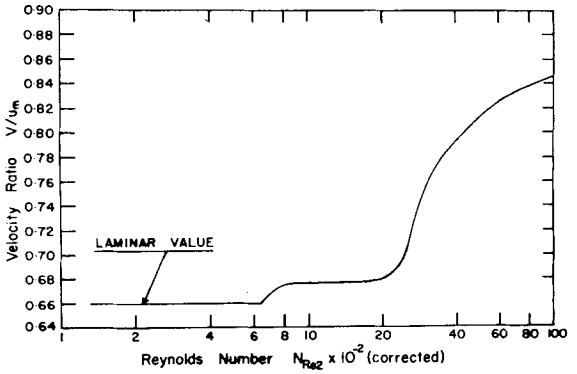

Fig. 5. Effect of Reynolds number on ratio of bulk average to maximum velocity for annulus with $r_1/r_2 = 0.33$.

EXPERIMENTAL RESULTS

The velocity profiles obtained in the transition range of flow are shown in Figures 1, 2, and 3. The ordinates are dimensional in feet per second, but the abscissae are dimensionless ratios. The symbols r_1 and r_2 denote the inner and outer radii of the annulus respectively. The distance r is the radius from the center of the whole configuration to the point of measurement in the fluid. The left boundary of each graph is therefore the outer wall of the annulus, and the right boundary is the surface of the core. The Reynolds numbers indicated on the separate curves are as defined in Equation (1) with r_m computed from Equation (3) as a matter of convenience.

Figure 4 summarizes the effect of Reynolds number on the radius of maximum velocity. Again the Reynolds number is the one used in the preceding figures. If the actual value of r_m were included in the Reynolds number, it would appear in both the ordinate and abscissa, a situation which is not desirable in this case. The circles represent the experimental velocity data; the solid line is the result of combining the pressure-drop data obtained in the present work with the core-side, skin-friction data of reference *4*. Since the latter authors experimented with an annulus of 0.337 radius ratio, their data can be applied directly to the present case with negligible error.

Figure 5 shows the experimentally determined relationship between the ratio of bulk average to maximum velocity V/u_m and the Reynolds number used in the preceding figures. The value of the bulk-average velocity is the one obtained directly from volumetric flow-rate measurements.

DISCUSSION AND RESULTS

The ordinates of Figures 1, 2, and 3 have been left in dimensional form to separate the curves on the graphs. It appears reasonable to assume however that the velocity ratio u/u_m is solely a function of Reynolds number N_{Re_2} and distance ratio $(r_2 - r)/(r_2 - r_1)$ in annuli having equal radius ratios r_1/r_2. On this basis point velocities can be predicted from the present data for annuli having $r_1/r_2 = 0.33$, even though they are not of the same absolute size as the experimental test section. If the bulk average velocity is known in such an annulus, the Reynolds number can be calculated and the velocity ratio V/u_m read from Figure 5. The maximum velocity can then be calculated immediately. Interpolation to the proper Reynolds number in Figure 1, 2, or 3 yields a unique velocity profile which can be reduced to a series of u/u_m values at the desired points in the fluid stream. The actual maximum velocity is then multiplied by these ratios to produce the velocity pattern for the case at hand.

Figure 4 shows remarkably good agreement between the experimental values of the radius of maximum velocity and those computed from frictional data. The drag measurements of reference *4* extend downward only to a Reynolds number of 1,500, and so it was necessary to use extrapolated values in the lower transition range. The extrapolation was based on the expectation of reaching fully viscous flow at a Reynolds number of about 700, since dye studies by Prengle and Rothfus (*2*) had suggested such a limit. As seen in Figure 4, the values of r_m obtained from the velocity profiles start to deviate from the laminar-flow position at a Reynolds number of 650. The friction factors calculated from the pressure-drop data of the present investigation also show a slight positive deviation from the laminar relationship, starting at about the same Reynolds number.

The radius of maximum velocity appears to shift toward the core in the lower transition zone and then to reverse its direction upon further increase in the Reynolds number. The outward progression takes r_m past its viscous-flow value and stops only when the lower critical Reynolds number of 2,200 is attained. This is the Reynolds number at which the friction factor at the outer wall reaches a minimum value and begins its sharp transitional increase. The authors of reference *2* have related this point to the casting off of the first large disturbance eddy. As the frequency of the disturbance eddies increases with further increase in Reynolds number, the radius of maximum velocity reapproaches its laminar value.

The friction factor at the outer wall indicates that the transition zone reaches its upper limit at a Reynolds number of about 3,100. Figure 4 shows that the radius of maximum velocity closely approaches the viscous-flow value given in Equation (3) at Reynolds numbers of 3,100 or more. Thus the deviation of r_m from the laminar value appears to be confined to the Reynolds number range in which frictional data show transitional behavior.

Figure 5 shows a sharp departure of the V/u_m curve from its viscous-flow value at the Reynolds number of 650. Another rapid change in slope occurs at the lower critical Reynolds number of 2,200 similar to the corresponding change at 2,100 Reynolds number in the case of smooth tubes. The Reynolds number is computed with r_m taken at its actual value. If the value of r_m obtained from from Equation (3) were used in the Reynolds number, its effect would be to shift the curve of Figure 5 to the left in the lower transition zone and to the right in the upper transition region. Since the maximum shifting amounts to only 9.4% decrease in the Reynolds number at the critical value of 2,200, the modification is slight in any range.

Smooth tubes and parallel plates can be considered to be limiting cases of annuli, as the radius ratio r_1/r_2 goes to zero and unity respectively. Since neither of these configurations demonstrates any lack of symmetry in the transition range, the observed shifting of the radius of maximum velocity must be a function of the radius ratio of the annulus. The friction factors computed from pressure-drop measurements show that the limits of the transition zone on the Reynolds-number scale are also functions of the radius ratio. The correlation of transitional velocities is therefore likely to be rather strongly dependent on r_1/r_2. Thus it is impractical to attempt a generalized correlation of transitional velocity patterns on the basis of data from one size of annulus. Further work on annuli of other radius ratios is currently in progress.

As an over-all check on the accuracy of the velocity data, the bulk average linear velocity of the stream was calculated by means of integration under the experimental profile. The result was compared with the corresponding flow rate determined directly by volumetric measurement. On the average the integrated velocities were 1.7% higher than the measured ones. The maximum deviation occurred at Reynolds numbers from 2,000 to 2,300 where the integrated velocities exceeded the measured values by about 3.5%. As differences of this magnitude are ordinary in such work, it can be concluded that the present data show no abnormal characteristics in this respect. Most of the error can be presumed to lie in the points nearest the bounding surfaces. Velocity probes calibrated in laminar flow usually read a few per cent too high in the region of a wall when the main flow is turbulent. It is also to be expected that local errors might be magnified to some extent in the transitional range. Since the local flow fluctuates over relatively long time intervals in this regime, the measurement of the time-mean local velocity is made more difficult than in fully laminar or fully turbulent flow.

NOTATION

f_1 = Fanning friction factor at inner surface of annulus, defined by Equation (4), dimensionless

f_2 = Fanning friction factor at outer surface of annulus, defined by Equation (2), dimensionless

g_c = conversion factor in Newton's second law of motion, equal to 32.2 (lb.-mass)(ft.)/(lb.-force)(sec.^{2})

N_{Re_2} = Reynolds number defined by Equation (1), dimensionless

r = radial distance from center of whole annular configuration to point of measurement in fluid, ft.

r_1 = radius of inner surface, or core, of annulus, ft.

r_2 = radius of outer surface of annulus, ft.

r_m = radius of maximum local fluid velocity, ft.

u = mean local fluid velocity, ft./sec.

u_m = maximum value of mean local fluid velocity, ft./sec.

V = bulk average linear fluid velocity, ft./sec.

Greek Letters

μ = viscosity of fluid, lb.-mass/(sec.)(ft.)

ρ = density of fluid, lb.-mass/cu. ft.

τ_1 = skin friction at inner surface of annulus, lb.-force/sq. ft.

τ_2 = skin friction at outer surface of annulus, lb.-force/sq. ft.

LITERATURE CITED

1. Knudsen, J. G., and D. L. Katz, "Proc. Midwestern Conf. Fluid Dynamics, 1st Conf.," No. 2, 175 (1950).
2. Prengle, R. S., and R. R. Rothfus, *Ind. Eng. Chem.*, **47**, 379 (1955).
3. Rothfus, R. R., C. C. Monrad, and V. E. Senecal, *ibid.*, **42**, 2511 (1950).
4. Rothfus, R. R., C. C. Monrad, K. G. Sikchi, and W. J. Heideger, *ibid.*, **47**, 913 (1955).
5. Rothfus, R. R., J. E. Walker, and G. A. Whan, *A.I.Ch.E. Journal*, **4**, 2 (1958).
6. Stanton, T. E., D. Marshall, and C. N. Bryant, *Proc. Roy. Soc. (London)*, **A97**, 413 (1920).
7. Walker, J. E., G. A. Whan, and R. R. Rothfus, *A.I.Ch.E. Journal*, **3**, (1957).

Manuscript received March 26, 1958; revision received July 3, 1958; paper accepted July 7, 1958.

Some Effects of Baffles on a Fluidized System

R. H. OVERCASHIER, D. B. TODD, and R. B. OLNEY

Shell Development Company, Emeryville, California

Some characteristics are reported for the fluidization of an air-microspheroidal catalyst system in a 16-in.-diameter bed equipped with baffles. The back-mixing characteristics and retention-time distributions of gas and solids, allowable gas and solids velocities, entrainment rate, and bed density are studied as functions of baffle design.

It is shown that the use of baffles narrows the retention-time spectrum and permits either concurrent or countercurrent flow while not seriously reducing gas or solids throughput or solids holdup.

For many reactions a fluidized-bed system offers important advantages, such as uniform temperatures under conditions of high heat release, large surface-to-volume ratio of the solids medium, and ease of transfer of the solids from one process vessel to another. The principal disadvantage of the fluid bed is its broad spectrum of gas and solids holding times. It has been shown that the residence-time spectrum of the fluid bed is much closer to that of a single well-mixed stage than to the more desirable infinite stages (piston flow). As reactor volume and the formation of unwanted by-products via consecutive reactions are both minimized by piston flow, this disadvantage can be serious.

The broad residence-time distribution of the conventional fluidized bed is well established. Singer, Todd, and Guinn (*5*) have shown that for the solids residence times used in commercial catalytic cracking (*5 to 40 min.*) the catalyst in each vessel could be regarded as perfectly mixed. The gas-retention-time studies of Gilliland, Mason, and Oliver (*2, 3*) in small columns showed that while the gas phase appeared neither well mixed nor in piston flow, it was much closer to the former. The present authors' measurements, shown in Figure 1 for a 16-in.-diam. fluid bed, confirm these previous findings. Gilliland, Mason, and Oliver postulated that the gas effluent from the bed results from the combination of two internal streams, one flowing slowly through the interstices of the solid and the other flowing rapidly via large bubbles or cavities containing very little solids. According to this analysis the majority of the gas travels via the rapidly moving bubbles and exchanges incompletely with the interstitial gas (that is, partially by-passes the bed). The resulting system effluent has a retention-time curve approximating the broad spectrum of a well-mixed stage. Similar findings are also reported by Handlos, Kunstman, and Schissler (*4*) for commercial fluidized beds.

If this analysis is correct, the bubbles play an important role in bed dynamics, providing both the density gradient which mixes the solids and the rapid escape path for part of the gas. They also appear inherent in the fluid bed, since they have been observed in many investigations, and their inevitability has been shown recently on theoretical grounds by Baron and Mugele (*1*). Thus the goal of narrowing the residence-time spectrum of the fluid bed appears to rest on minimizing the effect of the bubbles rather than on their elimination.

Many workers in the field of fluidization have suggested compartmenting the bed with horizontal baffles to narrow the residence-time spectrum. These baffles should narrow the spectrum by decreasing the velocity difference between the bubble and interstitial flows and by promoting transfer between them. In addition the baffles should impede the complete mixing of solids and result in staging of the solids flow, either for concurrent or countercurrent flow of solids and gas. Finally, since bubbles would still be present, the individual compartments would still have good heat-transfer characteristics.

The purpose of this investigation is to show the effect of horizontal baffles on the residence-time spectrum of solids and gas and on other characteristics of the fluid bed, such as allowable flow rates, mixture density, and solids entrainment. The experimental apparatus, operating techniques, and calculation